

Anion Directed Selective Synthesis of Supramolecular Metalloclusters and Related Coordination Dimers

Lisa Sturm,^[a] Christian R. Göb,^[a] and Iris M. Oppel*^[a]

The reaction of C_3 -symmetric *tris*-(2-pyridinylene-*N*-oxide) triaminoguanidinium salts ($[H_3L]X$) and zinc(II) in presence of thiocyanate and different carboxylate ions as co-ligands yields in a series of different coordination compounds. Supramolecular metalloclusters and carboxylate-bridged dimers are defined by two fundamentally different binding motifs. By adjusting the

co-ligands' stoichiometry, metalloclusters and carboxylate-bridged compounds can be synthesized selectively. Furthermore, the occupation of the metalloclusters with co-ligands can also be controlled that way. Directed synthesis of these metalloclusters is essential for further application in host-guest chemistry due to their cavities and porosity in the solid state.

Introduction

Over the last decades, supramolecular coordination chemistry has become a broad and diverse field benefitting from the variety of noncovalent intermolecular interactions.^[1] Coordination-driven self-assembly has proven to be an effective method for creating novel architectures up to formative practical applications.^[2] It allows for the preparation of highly complex supramolecular systems from relatively simple starting materials.^[3] Products are available via one-pot reactions and display physical properties that are generally inaccessible for organic species. Moreover, their reversible noncovalent bonds facilitate error checking and self-correction, making them superior to their organic counterparts in certain properties. Although some achievements within this field are initiated by serendipity, the recognition of similarities in the synthesis of different supramolecular assemblies allows prediction regarding the resulting structure.^[4] Well-defined coordination geometries of metal ions and individualized ligands enable the rational design of infinite networks like coordination polymers and metal-organic frameworks or discrete architectures.^[5] The latter include supramolecular cages with applications ranging from stabilization of reactive species^[6] and catalysis^[7] to sensors^[8] and drug delivery.^[9]

C_3 -symmetric triaminoguanidinium-based ligands combined with metal ions like cadmium(II), zinc(II) or palladium(II) were successfully implemented as triangular building blocks for the construction of supramolecular polyhedra like tetrahedron,^[10] octahedron^[11] and trigonal bipyramid^[12] (Figure 1a–c).^[13]

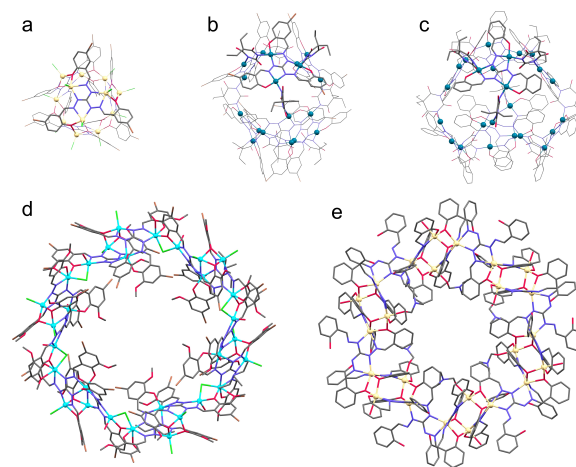


Figure 1. Crystal structures of selected supramolecular architectures from triaminoguanidinium-based ligands: tetrahedron $[(CdCl)_3(L'_6)]_4^{18-}$ (a),^[10b] trigonal bipyramid $[(Pd_3(L'_{Br}))_6(\mu\text{-bar})_3]^{12-}$ (b),^[12] octahedron $[(Pd_3L)_8(\mu\text{-bar})_{12}]^{16-}$ (c),^[11] and toroidal $[(Zn_2Cl(L'_{Br,OMe}))_2]_6(\mu\text{-Cl})_6(OH_2)_6]^{18-}$ (d)^[14] and $[(Cd_4(L'H_2)_2(L''H_2)(H_2O)(DMF))_6]^{16-}$ (e).^[15] Hydrogen atoms and counter ions are omitted, and equivalent entities are partly displayed thin for clarity.

Besides polyhedral architectures, a protein-sized toroidal coordination compound was observed consisting of twelve ligands and 30 zinc(II) ions (Figure 1d).^[14] The use of cadmium(II) ions causes triazole formation within the ligand under certain conditions, leading to a similarly shaped structure (Figure 1e).^[15] Although wheel-shaped architectures are common in polyoxometalate chemistry,^[16] such large toroidal coordination compounds are rather rare in literature.^[17] Due to their spacious and spheric cavity, a function as host for e.g. fullerene guests is conceivable.^[18]

Our group recently introduced a new type of toroidal, supramolecular metalloclusters whose cavities serve as excellent hosts for fullerenes C_{60} and C_{70} .^[18b] They are synthesized by self-assembly of pyridinyl-derived triaminoguanidinium-based ligands $[H_3L]X$ with three *tris*-chelating binding pockets in presence of zinc(II) and suitable co-ligands like chloride, bromide, thiocyanate or formate. The ligand's amine functions need to be deprotonated to provide chelating [NNO] binding

[a] L. Sturm, Dr. C. R. Göb, Prof. Dr. I. M. Oppel
Institute of Inorganic Chemistry
RWTH Aachen University
Landoltweg 1, 52074 Aachen, Germany
E-mail: iris.oppel@ac.rwth-aachen.de

Supporting information for this article is available on the WWW under <https://doi.org/10.1002/ejic.202001091>

© 2020 The Authors. European Journal of Inorganic Chemistry published by Wiley-VCH GmbH. This is an open access article under the terms of the Creative Commons Attribution License, which permits use, distribution and reproduction in any medium, provided the original work is properly cited.

pockets. Next to these metallocycles, coordination polymers were observed as byproducts in some cases. Their composition could not be analyzed yet. Recently, single crystals of coordination dimers and polymers were obtained which were suitable for X-ray diffraction. Their reaction environments hardly differ from the metallocycles', which arises the question of the structure-determining driving force. Addressing this issue is subject of this work.

Due to the dynamic and labile features of coordinative bonds, more than one species may be in equilibrium in solution if there is no clear thermodynamic preference for one species over the others.^[19] Environmental conditions like temperature, pressure as well as the reactants' concentrations control the thermodynamic equilibrium which was extensively investigated observing the self-assembly of 90° metal corners with linear and relatively rigid bridging ligands.^[20] Especially the relative stoichiometry may predefine the product's composition.^[21] Solvent-dependent supramolecular interactions and the polarity of the solvent play a fundamental role in the self-assembly of coordination compounds as well.^[22] Solvent coordination^[23] or inclusion^[24] may affect the product's structure beyond polarity effects.

Results and Discussion

To begin with, a particularly striking example was selected to illustrate the issue. The reaction of [H₃L]SCN and zinc(II) octanoate in dimethyl sulfoxide results in the crystallization of a metallocycle [Zn₆(OOCⁿHep)(NCS)₂L₃]₄ (**1**), but in the same reaction mixture differently shaped crystals of another coordination compound [Zn₄(μ-OOCⁿHep)₄(OOCⁿHep)(NCS)L₂] (**2**) were found (Figure 2).

Based on this result, two binding motifs are classified. Within the supramolecular metallocycle **1**, zinc(II) ions (light

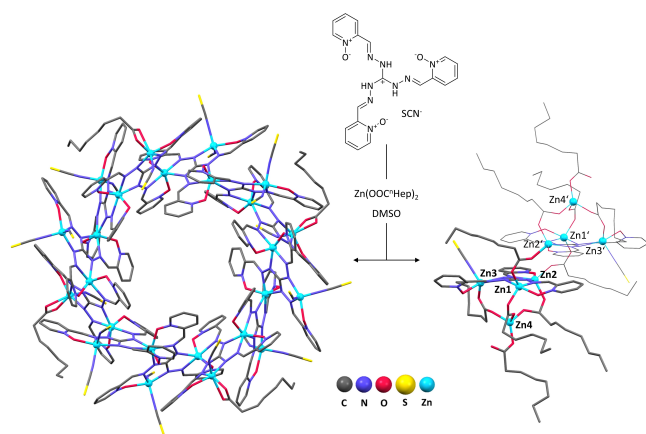


Figure 2. Metallocycle [Zn₆(OOCⁿHep)(NCS)₂L₃]₄ (**1**) and octanoate-bridged dimer [Zn₄(μ-OOCⁿHep)₄(OOCⁿHep)(NCS)L₂] (**2**) obtained through the reaction of [H₃L]SCN and zinc(II) octanoate in dimethyl sulfoxide. Zinc(II) ions are highlighted as spheres. Disordered solvent molecules were removed by the Squeeze routine (Platon).^[25] Hydrogen atoms and solvent molecules were omitted, and symmetry equivalent entities of the dimer are displayed thin for clarity.

blue) connect the ligands via octahedral coordination of two *tris*-chelating binding pockets, which allows cyclisation of the coordination oligomer after twelve subunits (Figure 3A, binding motif I). The charge of one zinc(II) ion is compensated by a deprotonated ligand L²⁻. ZnX₂ (dark blue) moieties occupy the twelve remaining [NNO] binding pockets. Chloride, bromide, thiocyanate and formate were already reported as co-ligands X⁻.^[18b]

The ligand connectivity in **2** compared to **1** differs fundamentally. Zn1 and Zn2 (light blue) are coordinated by a bridging carboxylate ion and one further co-ligand X⁻, giving a coordination number of five (Figure 3B, binding motif II). The carboxylate ion binds a second zinc(II) ion of the symmetrically equivalent entity (Zn2', Zn1'), building up an inversion centered dimer. As in binding motif I, ZnX₂ (dark blue) occupies the remaining binding pocket. Regarding compound **2**, Zn1-3 are capped by [Zn(OOCⁿHep)₄]²⁻ in order to compensate the charge.

The zinc(II) ratio in binding motif II is 1:3, whereas binding motif I provides a ligand to zinc(II) ratio of 1:2.

This experiment leads to the question why such different structures are formed in the same reaction environment. Which factors determine the binding motif? Is it possible to synthesize one structure type selectively?

To address these issues, the system needs to be simplified and the conditions kept as constant as possible in order to identify individual factors. Therefore, all the following experiments were performed under analogous reaction conditions at 22 °C in the same reaction vessels using similar amounts of solvent and comparable concentrations. Relatively weakly coordinating counter ions like nitrate and tetrafluoroborate were used for both the ligand and the zinc(II) salt in order to minimize the competition between different co-ligand species. As already mentioned, the ligand to zinc(II) ratio is 1:2 for binding motif I and 1:3 for binding motif II. However, the metallocycles in our earlier publication were obtained using a 1:3 ratio, which is why this ratio is kept for the following experiments, because it obviously does not influence the

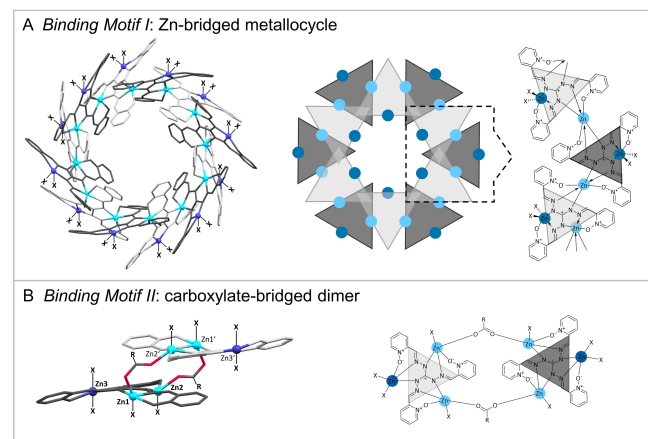


Figure 3. Generalized crystal structure and schematic representation of metallocycles (A, binding motif I) and carboxylate-bridged dimers (B, binding motif II) (X = co-ligands; R = H, alkyl). Zinc(II) ions are highlighted as spheres.

resulting structure type.^[18b] The identification and characterization of coordination compounds is mainly related to the solid phase, because structural elucidation by single-crystal X-ray diffraction is most reliable and ultimately a solid product is desired.

The metallocycle **1** contains significantly more thiocyanate ions than the carboxylate-bridged dimeric compound **2**. In a first step, the reaction was performed in absence of a thiocyanate source to investigate the influence of the pseudo-halide. The alkyl chain length of the carboxylate ion was varied from formate to propionate and two different solvents (dimethyl sulfoxide and *N,N*-dimethylformamide) were tested. Triethylamine was used stoichiometrically to deprotonate the ligand. The crystal structures of the resulting coordination compounds are shown in Figure 4.

Compounds **3**, **4**, and **6** crystallize from a reaction mixture containing $[H_3L]BF_4$ and the corresponding zinc(II) carboxylate in *N,N*-dimethylformamide, whereas **5** and **7** were found when dimethyl sulfoxide was used as solvent. The formula of **4–7** is generalized as $[Zn_3(\mu-OOCR)(OOCR)_3(solvent)L]_2$, where R describes the carboxylate chain length and the solvent is either a *N,N*-dimethylformamide or a dimethyl sulfoxide molecule. Hence, **4–7** differ only in the carboxylate chain length corresponding to the zinc(II) carboxylate used and the type of coordinated solvent molecule. These carboxylate-bridged

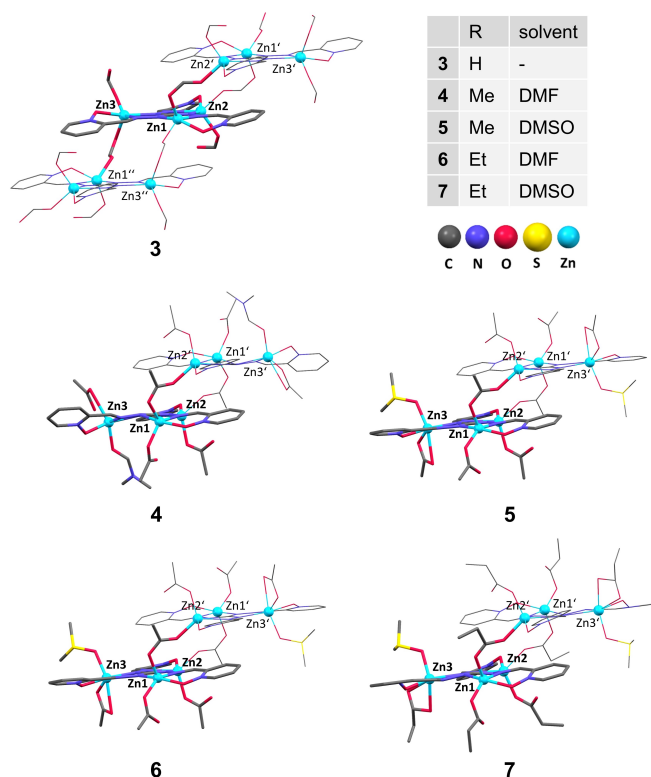


Figure 4. Crystal structures of $[Zn_3(\mu-OOCH)_2(OOCH)_2L]_n$ (**3**) and $[Zn_3(\mu-OOCR)(OOCR)_3(solvent)L]_2$ (**4**, **5**, **6**, **7**). Zinc(II) ions are highlighted as spheres. Disordered solvent molecules were removed by the Squeeze routine (Platon).^[25] Hydrogen atoms and free solvent molecules were omitted, and symmetry equivalent entities are displayed thin for clarity.

dination dimers follow binding motif II. Remaining coordination sites are occupied by six carboxylate ions and two solvent molecules for reasons of charge compensation.

$[Zn_3(\mu-OOCH)_2(OOCH)_2L]_n$ (**3**) is a coordination polymer containing formate co-ligands exclusively. The formation of a coordination polymer is probably most favorable. However, the polymer provides less space for co-ligands, so increasing the steric impact from formate (R=H) to acetate (R=Me) favors dimerization over polymerization already.

Characterization in solution is limited by solubility. Nevertheless, ESI-MS data and ¹H-NMR spectra of in dimethyl sulfoxide dissolved crystals indicate dynamic processes regarding depolymerization and co-ligand exchange.

The absence of a thiocyanate source results exclusively in formation of carboxylate-bridged compounds according to binding motif II. The carboxylate chain length only determines whether a coordination polymer or dimer crystallizes. The solvent does not affect the resulting binding motif either.

Binding motif II inevitably requires carboxylate to bridge the zinc(II) ions. As a second step, the carboxylate source was substituted by a thiocyanate salt. $[Zn_6(NCS)_6L_3]_4$ (**8**) crystallizes from a reaction mixture containing $[H_3L]NO_3$, zinc(II) tetrafluoroborate and sodium thiocyanate in *N,N*-dimethylformamide (Figure 5). It matches binding motif I, where thiocyanate is the only co-ligand X⁻.

In conclusion, the resulting binding motif obviously depends on the type of co-ligands. Using carboxylates leads to binding motif II, whereas thiocyanate causes the formation of supramolecular metallocycles according to binding motif I. Surprisingly, **1** and **2** contain both thiocyanate and octanoate.

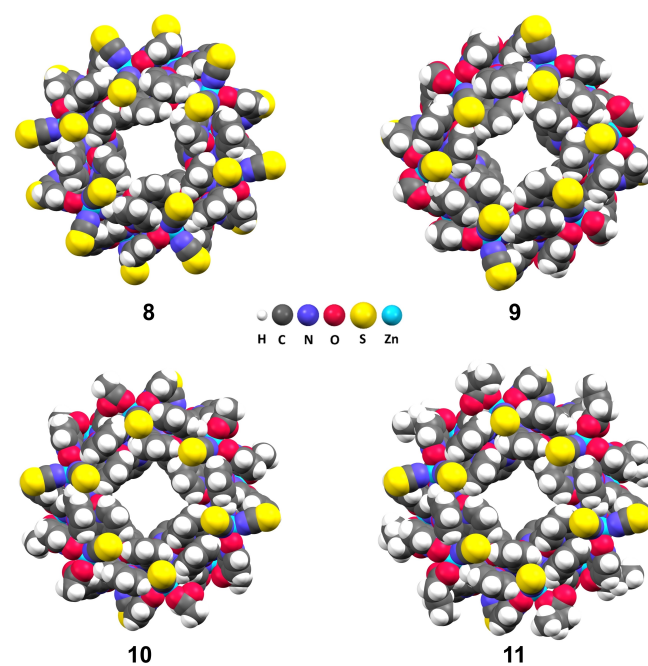


Figure 5. Metallocycles $[Zn_6(NCS)_6L_3]_4$ (**8**) and $[Zn_6(OOCR)_2(NCS)_4L_3]_4$ (**9**: R=H, **10**: R=Me, **11**: R=ⁿPr). Disordered solvent molecules were removed by the Squeeze routine (Platon).^[25]

As a third step, the experiment was performed in presence of both thiocyanate and different carboxylates in a 1:1 stoichiometry. To ensure a correct amount of carboxylate, they were formed *in situ* through deprotonation of the carboxylic acid by triethylamine. The base strength and stoichiometry were chosen to ensure both fully deprotonated carboxylic acid and ligand. $[\text{Zn}_6(\text{OOCH})_2(\text{NCS})_4\text{L}_3]_4$ (**9**), $[\text{Zn}_6(\text{OOCMe})_2(\text{NCS})_4\text{L}_3]_4$ (**10**), and $[\text{Zn}_6(\text{OOC}^n\text{Pr})_2(\text{NCS})_4\text{L}_3]_4$ (**11**) crystallize from a reaction mixture containing $[\text{H}_3\text{L}]\text{BF}_4$, zinc(II) tetrafluoroborate, sodium thiocyanate and the corresponding carboxylate in *N,N*-dimethylformamide. **9** was already published in our last work as an interesting host molecule for e.g. fullerenes. ^1H -DOSY-NMR spectroscopy already revealed neither decomposition nor aggregation of the metalocycles in solution.^[18b] Their solubility is closely related to their co-ligand occupation. However, due to the low symmetry within the compounds, even well-resolved data can barely be interpreted.

9 can be obtained from both dimethyl sulfoxide and *N,N*-dimethylformamide. As already reported, the solvent does not affect the formation of the dimers either, which is why only the latter solvent is tested here due to a shorter crystallization period and a higher crystal quality. The isostructural metalocycles **9**–**11** crystallize in the tetragonal space group $P4_21c$ with solvent filled channels along the crystallographic *c*-axis. The twelve remaining coordination sites are occupied by thiocyanate and carboxylate ions in a 2:1 ratio. Different carboxylate chain lengths only slightly alter the cell parameters.

9 can be obtained from both dimethyl sulfoxide and *N,N*-dimethylformamide. As already reported, the solvent does not affect the formation of the dimers either, which is why only the latter solvent is tested here due to a shorter crystallization period and a higher crystal quality. The isostructural metalocycles **9**–**11** crystallize in the tetragonal space group $P4_21c$ with solvent filled channels along the crystallographic *c*-axis. The twelve remaining coordination sites are occupied by thiocyanate and carboxylate ions in a 2:1 ratio. Different carboxylate chain lengths only slightly alter the cell parameters.

The presence of both types of co-ligands in a 1:1 stoichiometry resulted in isostructural metalocycles according to binding motif I. Since the octanoate-bridged dimer **2** also contains thiocyanate ions, there must be a critical thiocyanate to carboxylate ratio at which the system switches. To determine this critical ratio, different thiocyanate to carboxylate stoichiometries were screened. For this complex experiment, formate was chosen because it turned out to be most suitable for crystallization and characterization by X-ray diffraction. The crystalline compounds obtained from the reaction mixture of $[\text{H}_3\text{L}]\text{NO}_3$ and zinc(II) tetrafluoroborate in presence of different equivalents of sodium thiocyanate and *in situ*-formed formate in *N,N*-dimethylformamide are illustrated in Figure 6. They are identified by determining the cell parameters and symmetry via single-crystal X-ray diffraction (details in Table 1, SI). If both co-ligands are used in too low concentrations, no crystalline reaction product was obtained. Samples containing thiocyanate and formate in a $\geq 6:1$ ratio give metalocycle **8**, which contains thiocyanate exclusively. On the other side, samples containing thiocyanate and formate in a $\leq 1:6$ ratio with a maximum of one equivalent thiocyanate per ligand leads to the formate-bridged coordination polymer **3**. Increasing the formate amount to 1:12, 1:24, or 2:24 results in the formation of octahedral-shaped crystals of $[\text{Zn}_6(\text{OOCH})_5(\text{NCS})\text{L}_3]_4$ (**12**) next to prisms of **3**. The sample containing four equivalents thiocyanate and 24 equivalents formate provides exclusively crystals of **12**. Metallo-cycle **12** accords to binding motif I and differs from **9** only regarding the co-ligand occupation. It binds just four thiocyanate ions. The remaining sites are occupied by 20 formate ligands. However, compound **9** provides a thiocyanate to

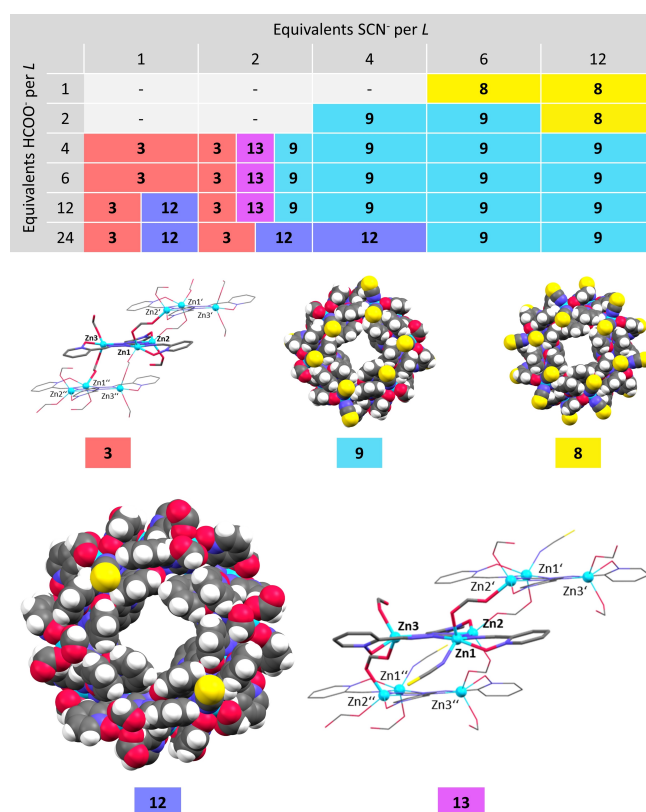


Figure 6. Table: Crystalline coordination compounds obtained from a reaction mixture of $[\text{H}_3\text{L}]\text{NO}_3$ and zinc(II) tetrafluoroborate in presence of different equivalents of sodium thiocyanate and *in situ*-formed formate in *N,N*-dimethylformamide, identified by determining the cell parameters and symmetry via single-crystal X-ray diffraction. Figures: Formate containing crystal structures of **3**, **8**, **9**, $[\text{Zn}_6(\text{OOCH})_5(\text{NCS})\text{L}_3]_4$ (**12**) and $[\text{Zn}_3(\mu\text{-OOCH})_2(\text{OOCH})(\text{NCS})\text{L}]_n$ (**13**). Zinc(II) ions are highlighted as spheres. Disordered solvent molecules were removed by the Squeeze routine (Platon).^[25] Partly, hydrogen atoms and free solvent molecules were omitted, and symmetry equivalent entities displayed thin for clarity.

formate ratio of 2:1. **12** crystallizes in another tetragonal space group $I\bar{4}$ with solvent filled channels along the crystallographic *c*-axis as well.

In the other samples containing two equivalents thiocyanate, three different types of crystals were distinguished: prisms of **3**, octahedrons of **9** and rods of $[\text{Zn}_3(\mu\text{-OOCH})_2(\text{OOCH})(\text{NCS})\text{L}]_n$ (**13**). Coordination polymer **13** is isostructural to **3**, except that Zn1 binds a thiocyanate instead of a formate ion.

The remaining samples with thiocyanate to formate ratios from 1:4 to 3:1 contained exclusively metalocycle **9**.

The fact that **8** forms at low formate and **3** at low thiocyanate amounts matches our previous observations because they only contain the respective other co-ligand. The comparison of samples with a thiocyanate to formate ratio of 1:6 all provides different results. 1:6 equivalents per ligand lead to crystallization of **3**, 2:12 equivalents give **3** next to **9** and **12** and 4:24 equivalents result in the formation of **12**. As a consequence, the resulting structure type does not only depend on the thiocyanate to formate ratio, but also on the ratio to ligand and zinc(II) ions as well.

Two equivalents thiocyanate per ligand can be identified as threshold because four different compounds were obtained in these samples. The formate-bridged polymer **3** crystallizes next to the isostructural polymer **13** containing one thiocyanate ion per subunit next to metallocycle **9**, which binds more thiocyanate than formate ions. Both binding motifs crystallize next to each other, whereby their crystallization affects the co-ligand concentrations in solution. These samples indicate the sensitivity of the system.

Metallocycle **12** is only obtained at a high formate stoichiometry and a maximum of four thiocyanate equivalents. High local formate concentrations are needed because it takes 20 formate ions to form this metallocycle. **9** is favored over a wide range and is not that sensitive towards changes regarding the thiocyanate to formate ratio.

Compounds **12** and **13** close the gap between mainly thiocyanate containing metallocycles of binding motif I and exclusively carboxylate containing dimers and polymers of binding motif II. Metallocycle **12** binds high amounts of formate and **13** is not exclusively occupied by formate. Consequently, the resulting structure type and so the binding motif sensitively depends on the stoichiometry of ligand, zinc(II), thiocyanate and carboxylate ions. Now that these ratios are identified, compounds **3**, **8**, **9**, and **12** can be synthesized selectively. This concept is probably transferable to further carboxylates besides formate, giving a wide range of structures.

The resulting binding motif is successfully attributed to the co-ligand stoichiometry. However, compound **1** and **2** were obtained in the same sample with the same amount of each reactant. The solution to this problem is the poor solubility of zinc(II) octanoate. Metallocycle **1** formed after two weeks and binds 20 thiocyanate and just four octanoate ions. Its crystallization reduces the thiocyanate concentration significantly. Dimer **2** crystallizes 5 months later. It binds just two thiocyanate ions. The relatively high zinc(II) octanoate concentration at this time is further indicated by the coordination of $[\text{Zn}(\text{OOC}^n\text{Hep})_4]^{2-}$ for reasons of charge compensation instead of two carboxylate ions and one solvent molecule as in **4**, **5**, **6** and **7**. Consequently, the formation of both binding motifs from the same reaction mixture is caused by the poor solubility of the zinc(II) salt and temporal changes in the reactant stoichiometry due to the crystallization of **1**.

Conclusion

With this work, the formation of supramolecular metallocycles is better understood because undefined byproducts are identified as coordination dimers and polymers. The ligand connectivity within these dimeric/polymeric structures is generalized as a second binding motif, fundamentally differing from the connectivity within the metallocycles. The reasons determining the binding motif are investigated. Solvent type and volume, reaction vessel, temperature and number of competitive anions are excluded by simplification and standardization of the system. The zinc to ligand ratio and the carboxylate chain length are neither crucial. The stoichiometry of thiocyanate and

carboxylate ions was identified as the structure determining driving force. Dimers, polymers, and metallocycles are synthesized selectively by adjusting the ratio of thiocyanate and carboxylate ions. The co-ligand occupation of the metallocycles is also controlled by the stoichiometry, so four new metallocycles are synthesized and characterized. All thiocyanate containing metallocycles crystallize in tetragonal space groups. In contrast to chloride or bromide containing metallocycles, which all crystallize in monoclinic space groups,^[18b] metallocycles crystallizing in tetragonal space groups possess channels through their cavities along the crystallographic *c*-axis. Metallocycle **9** was already identified as excellent host for fullerene guests like C_{60} and C_{70} .^[18b] The new metallocycles offer more opportunities for further host-guest chemistry. The electronic properties in- and outside the metallocycles change with the type of coordinating co-ligands, which was already verified by computations.^[18b] With this work, the metallocycles' polarity may be fine-tuned by the selective coordination of anions.

This work presented twelve new coordination compounds in sum, which are characterized by single-crystal and powder X-ray diffraction, ¹H-NMR spectroscopy, ESI mass spectrometry and IR-spectroscopy.

Experimental Section

Chemicals

Chemicals were used as received without further purification. 2-Formylpyridine-*N*-oxide,^[18b] triaminoguanidinium nitrate (TAG-NO_3)^[26] and the ligands $[\text{H}_3\text{L}]\text{SCN}$,^[18b] $[\text{H}_3\text{L}]\text{BF}_4$ ^[18b] and $[\text{H}_3\text{L}]\text{Cl}$ ^[18b] were synthesized according to published syntheses. The syntheses of TAG-OTf, $[\text{H}_3\text{L}]\text{OTf}$ and $[\text{H}_3\text{L}]\text{NO}_3$ were performed in an analogous manner (see further details in SI).

Zinc(II) carboxylates were obtained by refluxing an aqueous solution of basic zinc(II) carbonate and the respective carboxylic acid (see further details in SI).

Instrumentation and characterization

NMR spectra were measured on either a Bruker Avance II-400 or a Bruker Avance III HD at room temperature. The remaining proton signals of the solvents were used to reference the spectra according to tetramethylsilane (0 ppm).

Elemental analysis (C, H, N) was carried out at the Institute of Organic Chemistry, RWTH Aachen University, by Claudia Schleep on a Heraeus CHNO-Rapid VarioEL.

Electrospray-ionization mass spectrometry was performed on a ThermoFisher Scientific LTQ-Orbitrap XL at the Institute of Organic Chemistry, RWTH Aachen University, by Claudia Dittmer.

IR spectra were collected on a Nicolet Avatar 360 E.S.P. spectrometer. The samples were prepared as potassium bromide pellets by a hydraulic press.

X-ray powder diffraction experiments were performed by Tobias Storp at ambient temperature on flat samples with a Stoe and Cie STADI P diffractometer using germanium-monochromated $\text{Cu-K}_{\alpha 1}$ radiation ($\lambda = 1.54059 \text{ \AA}$). Compounds with large voids lose some of their crystallinity during drying.

Single crystal X-ray data were collected on a Bruker Apex-I CCD-diffractometer (Mo-K α , RWTH Aachen University), a Rigaku Supernova with an Atlas S2 CCD detector (Cu-K α , Ruhr-Universität Bochum), and a Stoe Stadivari with a Pilatus 3R 200 K detector (Cu-K α , RWTH Aachen University). The data was processed with the software packages provided by the manufacturers. Space groups were determined with XPREP (1997). The structures were solved either by a direct method with SHELXS (2013/1) or intrinsic phasing with SHELXT (2017/1). The structure refinement was carried out using SHELXL (2018/3) with a least-squares procedure against F 2 . Disordered solvent was treated with the SQUEEZE algorithm implemented in the software package PLATON (2018)^[25] or the BYPASS algorithm implemented in Olex2.^[27] Hydrogen atoms were calculated at their idealized positions and refined with a riding model. The isotropic displacement factors of aromatic and methylene hydrogen atoms were set to 1.2 times the displacement factors of the bound atoms and the methyl hydrogens were set to 1.5 times the displacement factors of the bound atoms.

Experimental details

[Zn $_6$ (OOCⁿHep)(NCS) $_5$ L $_3$] $_4$ (1). [H $_3$ L]SCN (10.0 mg, 20.9 μ mol, 1.0 eq.) and Zn(OOCⁿHep) $_2$ (22.1 mg, 62.8 μ mol, 3.0 eq.) were covered with dimethyl sulfoxide (0.5 mL) and heated until a clear solution was obtained. At 40 °C a stream of nitrogen was passed over the reaction mixture to slowly evaporate the solvent. Orange blocks of 1 crystallized after two weeks. After five months, orange rods of 2 crystallized next to orange blocks of 1.

[Zn $_4$ (μ -OOCⁿHep) $_4$ (OOCⁿHep)(NCS)L] $_2$ (2). [H $_3$ L]SCN (10.0 mg, 20.9 μ mol, 1.0 eq.) and Zn(OOCⁿHep) $_2$ (22.1 mg, 62.8 μ mol, 3.0 eq.) were covered with dimethyl sulfoxide (0.5 mL) and heated until a clear solution was obtained. At 40 °C a stream of nitrogen was passed over the reaction mixture to slowly evaporate the solvent. After five months, orange rods of 2 crystallized next to orange blocks of 1.

[Zn $_3$ (μ -OOCH) $_2$ (OOCH) $_2$ L] $_n$ (3). [H $_3$ L]NO $_3$ (5.0 mg, 10.4 μ mol, 1.0 eq.) was covered with solutions of Zn(BF $_4$) $_2$ hexahydrate (107.9 mg·mL $^{-1}$, 100 μ L, 3.0 eq.), triethylamine (283.1 mg·mL $^{-1}$, 33 μ L, 9 eq.), and formic acid (114.5 mg·mL $^{-1}$, 25 μ L, 6 eq.) in *N,N*-dimethylformamide and diluted with *N,N*-dimethylformamide (342 μ L). After two weeks at 22 °C, orange prisms crystallized. Yield: 6.0 mg, 4.0 μ mol, 62 %.

[Zn $_3$ (μ -OOCMe)(OOCMe) $_3$ (DMF)L] $_2$ (4). [H $_3$ L]BF $_4$ (10.0 mg, 19.7 μ mol, 1.0 eq.) and Zn(OOCMe) $_2$ dihydrate (13.0 mg, 59.1 μ mol, 3.0 eq.) were covered with a solution of triethylamine (22.5 mg·mL $^{-1}$, 500 μ L, 3.0 eq.) in *N,N*-dimethylformamide and diluted with *N,N*-dimethylformamide (500 μ L). After three weeks at 22 °C, yellow crystals were collected. Yield: 10.7 mg, 3.8 μ mol, 48 %.

[Zn $_3$ (μ -OOCMe)(OOCMe) $_3$ (DMSO)L] $_2$ (5). [H $_3$ L]OTf (12.5 mg, 21.9 μ mol, 1.0 eq.) and Zn(OOCMe) $_2$ dihydrate (14.4 mg, 65.5 μ mol, 3.0 eq.) were covered with dimethyl sulfoxide (0.7 mL). At 40 °C a slow stream of nitrogen was passed over the reaction mixture to slowly evaporate the solvent. Orange prisms were obtained after three months.

[Zn $_3$ (μ -OOCtEt)(OOCtEt) $_3$ (DMF)L] $_2$ (6). [H $_3$ L]BF $_4$ (10.0 mg, 19.7 μ mol, 1.0 eq.) and Zn(OOCtEt) $_2$ (12.5 mg, 59.1 μ mol, 3.0 eq.) were covered with a solution of triethylamine (22.5 mg·mL $^{-1}$, 500 μ L, 3.0 eq.) in dimethyl sulfoxide and diluted with dimethyl sulfoxide (500 μ L). Yellow plate-shaped crystals were collected after three weeks at 22 °C. Yield: 10.0 mg, 3.3 μ mol, 47 %.

[Zn $_3$ (μ -OOCtEt)(OOCtEt) $_3$ (DMSO)L] $_2$ (7). [H $_3$ L]BF $_4$ (10.0 mg, 19.7 μ mol, 1.0 eq.) and Zn(OOCtEt) $_2$ (12.5 mg, 59.1 μ mol, 3.0 eq.) were covered with a solution of triethylamine (22.5 mg·mL $^{-1}$, 500 μ L, 3.0 eq.) in *N,N*-dimethylformamide and diluted with *N,N*-dimethylformamide

(500 μ L). Yellow rod-shaped crystals were collected after three weeks at 22 °C. Yield: 14.0 mg, 4.1 μ mol, 62 %.

[Zn $_6$ (NCS) $_6$ L $_3$] $_4$ (8). [H $_3$ L]NO $_3$ (5.0 mg, 10.36 μ mol, 1.0 eq.) was covered with solutions of Zn(BF $_4$) $_2$ hexahydrate (107.9 mg·mL $^{-1}$, 100 μ L, 3.0 eq.), triethylamine (283.1 mg·mL $^{-1}$, 11 μ L, 3.0 eq.), and NaSCN (100.8 mg·mL $^{-1}$, 50 μ L, 6.0 eq.) in *N,N*-dimethylformamide and diluted with *N,N*-dimethylformamide (339 μ L). Orange crystals were obtained after one week at 22 °C.

[Zn $_6$ (OOCMe) $_2$ (NCS) $_4$ L $_3$] $_4$ (10). [H $_3$ L]BF $_4$ (10.0 mg, 19.7 μ mol, 1.0 eq.) and Zn(BF $_4$) $_2$ hexahydrate (20.5 mg, 59.1 μ mol, 3.0 eq.), NaOOCMe (4.8 mg, 59.1 μ mol, 3.0 eq.), and NaSCN (4.8 mg, 59.1 μ mol, 3.0 eq.) were covered with *N,N*-dimethylformamide (1.0 mL). Orange octahedral shaped crystals were collected after two weeks at 22 °C. Yield: 7.7 mg, 0.61 μ mol, 45 %.

[Zn $_6$ (OOCⁿPr) $_2$ (NCS) $_4$ L $_3$] $_4$ (11). [H $_3$ L]BF $_4$ (10.0 mg, 19.7 μ mol, 1.0 eq.) and Zn(BF $_4$) $_2$ hexahydrate were covered with triethylamine (41.1 μ L, 295.7 μ mol, 15.0 eq.) and solutions of butyric acid (41.7 mg·mL $^{-1}$, 125 μ L, 3.0 eq.) and NaSCN (19.2 mg·mL $^{-1}$, 250 μ L, 3.0 eq.) in *N,N*-dimethylformamide and diluted with *N,N*-dimethylformamide (625 μ L). Orange octahedral shaped crystals were collected after one month at 22 °C. Yield: 4.9 mg, 0.39 μ mol, 29 %.

[Zn $_6$ (OOCH) $_5$ (NCS)L $_3$] $_4$ (12). [H $_3$ L]NO $_3$ (5.0 mg, 10.4 μ mol, 1.0 eq.) was covered with solutions of Zn(BF $_4$) $_2$ hexahydrate (107.9 mg·mL $^{-1}$, 100 μ L, 3.0 eq.), NaSCN (100.8 mg·mL $^{-1}$, 25.0 μ L, 4.0 eq.), formic acid (114.5 mg·mL $^{-1}$, 100 μ L, 24.0 eq.) and triethylamine (283.1 mg·mL $^{-1}$, 100 μ L, 27.0 eq.) in *N,N*-dimethylformamide and filled up to 500 μ L with *N,N*-dimethylformamide. Orange octahedral shaped crystals were collected after two weeks at 22 °C. Yield: 2.0 mg, 0.17 μ mol, 24 %.

[Zn $_3$ (μ -OOCH) $_2$ (OOCH)(NCS)L] $_n$ (13). [H $_3$ L]NO $_3$ (5.0 mg, 10.4 μ mol, 1.0 eq.) was covered with solutions of Zn(BF $_4$) $_2$ hexahydrate (107.9 mg·mL $^{-1}$, 100 μ L, 3.0 eq.), NaSCN (100.8 mg·mL $^{-1}$, 17 μ L, 2.0 eq.), formic acid (114.5 mg·mL $^{-1}$, 17 μ L, 4.0 eq.) and triethylamine (283.1 mg·mL $^{-1}$, 26 μ L, 7.0 eq.) in *N,N*-dimethylformamide and filled up to 500 μ L with *N,N*-dimethylformamide. After one month at 22 °C, yellow rods of 13 crystallized next to orange octahedral shaped crystals of 9 and orange prisms of 3.

Corresponding analytical and crystallographic data are shown in the SI.

CCDC 2025630, 2025629, 2025695, 2025700, 2025632, 2025699, 2025697, 2025631, 2025696, 2025698, 2025694, 2025693 (1, 2, 3, 4, 5, 6, 7, 8, 10, 11, 12, 13 respectively), contain the supplementary crystallographic data for this paper. These data are provided free of charge by The Cambridge Crystallographic Data Centre.

Acknowledgements

We gratefully acknowledge the RWTH Aachen University (Graduiertenförderung) and the International Research Training Group 1628 SeleCa "Selectivity in Chemo- and Bio-catalysis" (Deutsche Forschungsgemeinschaft) for funding this work. Furthermore, we like to thank Dr. Khai Nghi Truong from the group of Prof. Dr. Ullrich Englert (RWTH Aachen University) and Manuela Winter (Lehrstuhl für Anorganische Chemie II, Ruhr-Universität Bochum) for collecting single-crystal X-ray diffraction data. Open access funding enabled and organized by Projekt DEAL.

Conflict of Interest

The authors declare no conflict of interest.

Keywords: Supramolecular chemistry · Self-assembly · Zinc · X-ray diffraction

- [1] J. M. Lehn, *Chem. Soc. Rev.* **2017**, *46*, 2378–2379.
- [2] T. R. Cook, P. J. Stang, *Chem. Rev.* **2015**, *115*, 7001–7045.
- [3] B. H. Northrop, Y. R. Zheng, C. H. I. Ki-Whan, P. J. Stang, *Acc. Chem. Res.* **2009**, *42*, 1554–1563.
- [4] a) R. W. Saalfrank, H. Maid, A. Scheurer, *Angew. Chem. Int. Ed.* **2008**, *47*, 8794–8824; *Angew. Chem.* **2008**, *120*, 8924–8956; b) B. J. Holliday, C. A. Mirkin, *Angew. Chem. Int. Ed.* **2001**, *40*, 2022–2043; *Angew. Chem.* **2001**, *113*, 2076–2097; c) R. Chakrabarty, P. S. Mukherjee, P. J. Stang, *Chem. Rev.* **2011**, *111*, 6810–6918.
- [5] T. R. Cook, Y. R. Zheng, P. J. Stang, *Chem. Rev.* **2013**, *113*, 734–777.
- [6] a) M. Yoshizawa, T. Kusukawa, M. Fujita, S. Sakamoto, K. Yamaguchi, *J. Am. Chem. Soc.* **2001**, *123*, 10454–10459; b) Y. Kohyama, T. Murase, M. Fujita, *Chem. Commun.* **2012**, *48*, 7811–7813; c) M. Ziegler, J. L. Brumaghim, K. N. Raymond, *Angew. Chem. Int. Ed.* **2000**, *39*, 4119–4121; *Angew. Chem.* **2000**, *112*, 4285–4287; d) A. Galan, P. Ballester, *Chem. Soc. Rev.* **2016**, *45*, 1720–1737.
- [7] a) D. Samanta, S. Mukherjee, Y. P. Patil, P. S. Mukherjee, *Chem. Eur. J.* **2012**, *18*, 12322–12329; b) C. J. Hastings, R. G. Bergman, K. N. Raymond, *Chem. Eur. J.* **2014**, *20*, 3966–3973; c) C. W. Zhao, J. P. Ma, Q. K. Liu, Y. Yu, P. Wang, Y. A. Li, K. Wang, Y. Bin Dong, *Green Chem.* **2013**, *15*, 3150–3154; d) M. Otte, P. F. Kuijpers, O. Troeppner, I. Ivanovic-Burmazovic, J. N. H. Reek, B. De Bruin, *Chem. Eur. J.* **2013**, *19*, 10170–10178; e) W. Brenner, T. K. Ronson, J. R. Nitschke, *J. Am. Chem. Soc.* **2017**, *139*, 75–78; f) C. Tan, D. Chu, X. Tang, Y. Liu, W. Xuan, Y. Cui, *Chem. Eur. J.* **2019**, *25*, 662–672.
- [8] a) J. Wang, C. He, P. Wu, J. Wang, C. Duan, *J. Am. Chem. Soc.* **2011**, *133*, 12402–12405; b) C. He, J. Wang, P. Wu, L. Jia, Y. Bai, Z. Zhang, C. Duan, *Chem. Commun.* **2012**, *48*, 11880–11882; c) H. Ahmad, B. W. Hazel, A. J. H. M. Meijer, J. A. Thomas, K. A. Wilkinson, *Chem. Eur. J.* **2013**, *19*, 5081–5087; d) J. Dong, Y. Zhou, F. Zhang, Y. Cui, *Chem. Eur. J.* **2014**, *20*, 6455–6461.
- [9] a) M. J. Webber, R. Langer, *Chem. Soc. Rev.* **2017**, *46*, 6600–6620; b) Y. Cai, H. Shen, J. Zhan, M. Lin, L. Dai, C. Ren, Y. Shi, J. Liu, J. Gao, Z. Yang, *J. Am. Chem. Soc.* **2017**, *139*, 2876–2879; c) I. V. Grishagin, J. B. Pollock, S. Kushal, T. R. Cook, P. J. Stang, B. Z. Olenyuk, *Proc. Natl. Acad. Sci. USA* **2014**, *111*, 18448–18453; d) I. V. Kolesnichenko, E. V. Anslyn, *Chem. Soc. Rev.* **2017**, *46*, 2385–2390.
- [10] a) I. M. Müller, R. Robson, F. Separovic, *Angew. Chem. Int. Ed.* **2001**, *40*, 4385–4386; *Angew. Chem.* **2001**, *113*, 4519–4520; b) I. M. Müller, D. Möller, C. A. Schalley, *Angew. Chem. Int. Ed.* **2005**, *44*, 480–484; *Angew. Chem.* **2005**, *117*, 485–488; c) I. M. Oppel, K. Föcker, *Angew. Chem. Int. Ed.* **2008**, *47*, 402–405; *Angew. Chem.* **2008**, *120*, 408–411.
- [11] I. M. Müller, S. Spillmann, H. Franck, R. Pietschnig, *Chem. Eur. J.* **2004**, *10*, 2207–2213.
- [12] I. M. Müller, D. Möller, *Angew. Chem. Int. Ed.* **2005**, *44*, 2969–2973; *Angew. Chem.* **2005**, *117*, 3029–3033.
- [13] C. von Eßen, C. R. Göb, I. M. Oppel, in *Guanidines as Reagents Catal. II (Ed. P. Selig)*, Springer, **2015**, pp. 75–94.
- [14] I. M. Müller, D. Möller, K. Föcker, *Chem. Eur. J.* **2005**, *11*, 3318–3324.
- [15] I. M. Müller, R. Robson, *Angew. Chem. Int. Ed.* **2000**, *39*, 4357–4359; *Angew. Chem.* **2000**, *112*, 4527–4530.
- [16] a) T. Liu, E. Diemann, H. Li, A. W. M. Dress, A. Müller, *Nature* **2003**, *426*, 59–62; b) S. Polarz, B. Smarsly, M. Antonietti, *ChemPhysChem* **2001**, *2*, 457–461; c) W. Xuan, R. Pow, Q. Zheng, N. Watfa, D. L. Long, L. Cronin, *Angew. Chem. Int. Ed.* **2019**, *58*, 10867–10872; d) E. Garrido Ribó, N. L. Bell, W. Xuan, J. Luo, D. L. Long, T. Liu, L. Cronin, *J. Am. Chem. Soc.* **2020**, *142*, 17508–17514; e) P. Kögerler, L. Cronin, *Angew. Chem. Int. Ed.* **2005**, *44*, 844–846; *Angew. Chem.* **2005**, *117*, 866–868; f) O. Botezat, J. Van Leusen, V. C. Kravtsov, P. Kögerler, S. G. Baca, *Inorg. Chem.* **2017**, *56*, 1814–1822; g) S. S. Mal, U. Kortz, *Angew. Chem. Int. Ed.* **2005**, *44*, 3777–3780; *Angew. Chem.* **2005**, *117*, 3843–3846; h) A. J. Tasiopoulos, A. Vinslava, W. Wernsdorfer, K. A. Abboud, G. Christou, *Angew. Chem. Int. Ed.* **2004**, *43*, 2117–2121; *Angew. Chem.* **2004**, *116*, 2169–2173.
- [17] a) J. Langer, S. Maitland, S. Grams, A. Ciucka, J. Pahl, H. Elsen, S. Harder, *Angew. Chem.* **2017**, *129*, 5103–5107; *Angew. Chem. Int. Ed.* **2017**, *56*, 5021–5025; b) R. Akiyoshi, K. Kuroiwa, M. Sakuragi, S. Yoshimoto, R. Ohtani, M. Nakamura, L. F. Lindoy, S. Hayami, *Chem. Commun.* **2020**, *56*, 5835–5838.
- [18] a) S. Kawano, T. Fukushima, K. Tanaka, *Angew. Chem.* **2018**, *130*, 15043–15047; b) C. R. Göb, A. Ehnbohm, L. Sturm, Y. Tobe, I. M. Oppel, *Chem. Eur. J.* **2020**, *26*, 3609–3613.
- [19] W. Wang, Y. X. Wang, H. B. Yang, *Chem. Soc. Rev.* **2016**, *45*, 2656–2693.
- [20] a) M. Fujita, O. Sasaki, T. Mitsunashi, T. Fujita, J. Yazaki, K. Yamaguchi, K. Ogura, *Chem. Commun.* **1996**, *20*, 1535–1536; b) M. Ferrer, A. Gutiérrez, M. Mounir, O. Rossell, E. Ruiz, A. Rang, M. Engeser, *Inorg. Chem.* **2007**, *46*, 3395–3406; c) E. Holló-Sitkei, G. Tárkányi, L. Párkányi, T. Megyes, G. Besenyey, *Eur. J. Inorg. Chem.* **2008**, 1573–1583; d) K. Uehara, K. Kasai, N. Mizuno, *Inorg. Chem.* **2010**, *49*, 2008–2015.
- [21] a) J. Lee, K. Ghosh, P. J. Stang, *J. Am. Chem. Soc.* **2009**, *131*, 12028–12029; b) S. Hiraoka, T. Yi, M. Shiro, M. Shionoya, *J. Am. Chem. Soc.* **2002**, *124*, 14510–14511; c) S. Hiraoka, K. Harano, M. Shiro, M. Shionoya, *Angew. Chem.* **2005**, *117*, 2787–2791; *Angew. Chem. Int. Ed.* **2005**, *44*, 2727–2731; d) K. Harano, S. Hiraoka, M. Shionoya, *J. Am. Chem. Soc.* **2007**, *129*, 5300–5301; e) A. Chakraborty, L. Srinivasa Rao, A. K. Manna, S. K. Pati, J. Ribas, T. K. Maji, *Dalton Trans.* **2013**, *42*, 10707–10714; f) S. Yuan, H. Wang, D. X. Wang, H. F. Lu, S. Y. Feng, D. Sun, *CrystEngComm* **2013**, *15*, 7792–7802.
- [22] a) M. Asakawa, G. Brancato, M. Fantì, D. A. Leigh, T. Shimizu, A. M. Z. Slawin, J. K. Y. Wong, F. Zerbetto, S. Zhang, *J. Am. Chem. Soc.* **2002**, *124*, 2939–2950; b) B. Kilbas, S. Mirtschin, R. Scopelliti, K. Severin, *Chem. Sci.* **2012**, *3*, 701–704; c) O. Gidron, M. Jirásek, N. Trapp, M. O. Ebert, X. Zhang, F. Diederich, *J. Am. Chem. Soc.* **2015**, *137*, 12502–12505.
- [23] a) J. Lu, T. Paliwala, S. C. Lim, C. Yu, T. Niu, A. J. Jacobson, *Inorg. Chem.* **1997**, *36*, 923–929; b) O. S. Jung, S. H. Park, K. M. Kim, H. G. Jang, *Inorg. Chem.* **1998**, *37*, 5781–5785; c) K. Ohara, M. Tominaga, I. Azumaya, K. Yamaguchi, *Anal. Sci.* **2013**, *29*, 773–776; d) J. Ramírez, A. M. Stadler, N. Kyriatsakas, J. M. Lehn, *Chem. Commun.* **2007**, 237–239.
- [24] a) P. N. W. Baxter, R. G. Khoury, J. M. Lehn, G. Baum, D. Fenske, *Chem. Eur. J.* **2000**, *6*, 4140–4148; b) K. Suzuki, M. Kawano, M. Fujita, *Angew. Chem.* **2007**, *119*, 2877–2880; *Angew. Chem. Int. Ed.* **2007**, *46*, 2819–2822.
- [25] A. L. Spek, *Acta Crystallogr. Sect. C* **2015**, *71*, 9–18.
- [26] S. Weiss, H. Krommer, Process for the preparation of triaminoguanidine salts, Patent DE3341645 A1, **1985**.
- [27] O. V. Dolomanov, L. J. Bourhis, R. J. Gildea, J. A. K. Howard, H. Puschmann, *J. Appl. Crystallogr.* **2009**, *42*, 339–341.

Manuscript received: December 2, 2020

Revised manuscript received: December 20, 2020

Accepted manuscript online: December 22, 2020